Cold-Atom Temporally Multiplexed Quantum Memory with Cavity-Enhanced Noise Suppression

Lukas Heller,[1,*] Pau Farrera,[1,†] Georg Heinze,[1,‡] and Hugues de Riedmatten[1,2,§]
[1]ICFO-Institut de Ciencies Fotoniques, The Barcelona Institute of Science and Technology, 08860 Castelldefels (Barcelona), Spain
[2]ICREA-Institució Catalana de Recerca i Estudis Avançats, 08015 Barcelona, Spain

(Received 14 November 2019; accepted 27 April 2020; published 28 May 2020)

Future quantum repeater architectures, capable of efficiently distributing information encoded in quantum states of light over large distances, will benefit from multiplexed photonic quantum memories. In this work we demonstrate a temporally multiplexed quantum repeater node in a laser-cooled cloud of ^{87}Rb atoms. We employ the Duan-Lukin-Cirac-Zoller protocol where pairs of photons and single collective spin excitations (so-called spin waves) are created in several temporal modes using a train of write pulses. To make the spin waves created in different temporal modes distinguishable and enable selective readout, we control the dephasing and rephasing of the spin waves by a magnetic field gradient, which induces a controlled reversible inhomogeneous broadening of the involved atomic hyperfine levels. We demonstrate that by embedding the atomic ensemble inside a low finesse optical cavity, the additional noise generated in multimode operation is strongly suppressed. By employing feed forward readout, we demonstrate distinguishable retrieval of up to 10 temporal modes. For each mode, we prove nonclassical correlations between the first and second photon. Furthermore, an enhancement in rates of correlated photon pairs is observed as we increase the number of temporal modes stored in the memory. The reported capability is a key element of a quantum repeater architecture based on multiplexed quantum memories.

DOI: 10.1103/PhysRevLett.124.210504

Quantum light-matter interfaces are key platforms in the field of quantum information. They provide storage, processing, or synchronization of photonic quantum states, which can be used for applications in quantum communication, computation, or sensing [1,2]. One example is optical quantum memories, devices able to store and retrieve photonic quantum states. Multiplexed optical quantum memories are important in order to achieve higher data communication rates, as it is similarly done in conventional classical communications. One particularly interesting application of multiplexed quantum memories is to enhance the entanglement distribution rate in quantum repeaters [3], which in turn also facilitate their practical realization by relaxing the storage time requirements. For this application, the quantum memory should be able to store a large number of distinguishable modes and to read them out selectively. Different degrees of freedom have been considered for the multiplexed modes, such as frequency, space, or time. Ensemble-based platforms, where photonic quantum information is mapped onto collective atomic excitations, are well suited for demonstrating quantum information multiplexing.

Cold atomic gases are currently one of the best quantum memory platforms with excellent properties demonstrated, including single photon storage and retrieval efficiency up to 90% [4–8] and storage time up to 220 ms [5,9]. In particular, this system is well suited for realizing a photon pair source with embedded quantum memory following the Duan-Lukin-Cirac-Zoller (DLCZ) protocol [10], that can be used as a quantum repeater node [11–13]. Current multimode atomic memories focus mainly on spatial multiplexing, e.g., addressing modes with different wave vectors or multiple memory cells in different parts of the cloud [14–20]. Beyond spatial multiplexing, time multiplexing provides a practical way to store multiple distinguishable modes in the same ensemble of atoms. So far, time multiplexing has been mostly studied in solid-state quantum memories based on inhomogeneously broadened rare-earth doped crystals, using the atomic frequency comb scheme [21–32]. In contrast, very few experiments have investigated time multiplexing in atomic gases either by using a controlled and reversible broadening of the spin transition [33–36] or very recently by mapping photons generated in different spatial modes to different temporal modes [37,38].

Previous attempts to generate nonclassically correlated pairs of photons and spin waves in multiple temporal modes in the same spatial mode have been plagued by a linear increase of the noise as a function of number of modes due to dephased spin waves [35]. This effect prevents significant gain in photon pair generation rate, compared to the single-mode case. In this Letter, following a proposal by Simon *et al.* [39], we demonstrate that by embedding the ensemble inside a low finesse cavity, one can substantially reduce noise from dephased spin waves. We experimentally show noise reduction by a factor of 14. Subsequently, we demonstrate the generation of

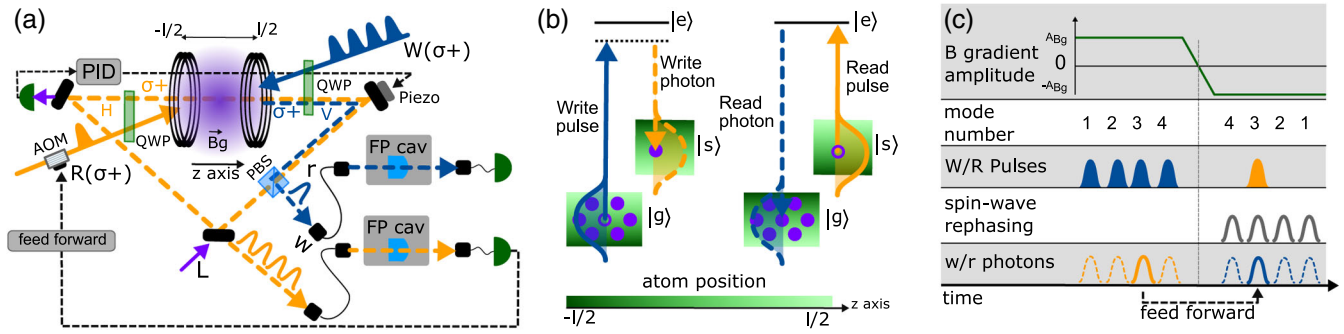

FIG. 1. (a) Schematic overview of the experimental setup. W, write pulse; R, read pulse; w, write photon; r, read photon; L, cavity locking laser beam; PID, proportional-integral-derivative controller; FP cav, Fabry-Perot filtering optical cavity; l, atomic cloud length; QWP, quarter-wave plate; PBS, polarization beam splitter, AOM, acousto-optic modulator; Bg, magnetic field gradient. The polarizations indicated are in the atomic frame (cf. Ref. [40]). (b) Energy levels relevant for the photon generation process. The green color gradient bars illustrate the position dependent Zeeman level energy shift along the z axis. (c) Time diagram of events occurring in the temporally multiplexed operation of the system. In this example, 4 write pulse modes are sent to the atomic cloud. A magnetic field gradient of amplitude A_{Bg} is present which is reversed to $-A_{\mathrm{Bg}}$ after the last write pulse mode. If a write photon is detected in the third mode, a feed forward instruction sends the read pulse at the time corresponding to the third-mode spin wave rephasing time.

cavity-enhanced photons paired with spin waves in up to 10 temporal modes while preserving high quantum correlations between the photons and spin waves. This allows us to increase the spin wave–photon (photon pair) creation rate by a factor of 10 (7.3), with respect to the single-mode case. The number of modes could be greatly improved by increasing the finesse of the cavity.

In the DLCZ scheme, an off-resonant write laser pulse generates collective excitations in an atomic cloud that are correlated with Raman scattered write photons. These excitations can be mapped with high readout efficiency into read photons as long as the atomic coherence is preserved. In order to achieve temporal multiplexing, we need two additional ingredients: first, controlled dephasing and rephasing of the collective excitations that allows one to distinguish spin waves created at different temporal modes, and second, an optical cavity to reduce noise generated from the dephased excitation modes [39].

The experimental setup is shown in Fig. 1(a). We cool an ensemble of ^{87}Rb atoms in a magneto-optical trap to a temperature of around 40 μK. The relevant atomic levels are shown in Fig. 1(b) and consist of two metastable ground states ($|g\rangle = |5^2S_{1/2}, F = 1, m_F = 1\rangle$ and $|s\rangle = |5^2S_{1/2}, F = 2, m_F = 1\rangle$) and one excited state ($|e\rangle = |5^2P_{3/2}, F = 2, m_F = 2\rangle$). After optically pumping the atoms to $|g\rangle$, a write pulse with duration $\Delta t_W = 266$ ns drives the transition $|g\rangle \rightarrow |e\rangle$ red detuned by $\Delta = 40$ MHz. This process probabilistically generates write photons on the $|e\rangle \rightarrow |s\rangle$ transition through spontaneous Raman scattering that are paired with collective spin excitations (atoms in $|s\rangle$).

In order to distinguish different spin wave temporal modes, a spatial gradient magnetic field is present during writing. This causes a position dependent energy shift of the atomic levels through the Zeeman effect. The temporal evolution of the spin waves can be written as

$$|\Psi_a(t)\rangle = \frac{1}{\sqrt{N}} \sum_{j=1}^{N} e^{i\mathbf{x}_j(\mathbf{k}_W - \mathbf{k}_w) + i\int_0^t \Delta w_j(t')dt'} |g_1 \ldots s_j \ldots g_N\rangle, \tag{1}$$

where the two-photon detuning Δw_j is different for each atom. Here, N denotes the total number of atoms, $\mathbf{x}_j$ the initial atom position, and $\mathbf{k}_{W(w)}$ the wave vector of the write pulse (photon). $\Delta w_j = \mu_B B(x_j)(g_{F(|s\rangle)} m_{F(|s\rangle)} - g_{F(|g\rangle)} m_{F(|g\rangle)})/\hbar$, where μ_B is the Bohr magneton, $B(x_j)$ is the magnetic field at the position of atom j, $g_{F(|s,g\rangle)}$ is the Landé g factor, and $m_{F(|s,g\rangle)}$ the quantum number corresponding to the z component of the total angular momentum. The gradient field is provided by the trapping coils.

The collective atomic excitation can be converted into a read photon by means of a read pulse resonant to the $|s\rangle \rightarrow |e\rangle$ transition. In the absence of atomic dephasing the emission will be highly efficient into a particular spatio-temporal mode thanks to collective interference of all contributing atoms. In the case of spin wave dephasing, i.e., like the one induced by the magnetic field gradient, no collective interference occurs and the readout process will not be efficient. However, inverting the amplitude of the magnetic field gradient (and thereby inverting the phase evolution of the spin wave) eventually leads to its rephasing and efficient photon retrieval. This technique can be used to write N_m different temporal modes and select a particular one to be read out [see Fig. 1(c)]. Note that while we can trigger the phase reversal on demand, there will be a delay between this trigger and the actual readout. This delay does not prevent however the use of our memory in a quantum repeater architecture, as explained in the Supplemental Material [40].

When reading a particular temporal mode, a major noise source arises from dephased spin waves generated in other

temporal modes. During writing, spin waves are created which are paired with photons emitted into all possible modes, not only the write photon mode. Such spin waves, if in phase, emit read photons into the corresponding phase matched (uncollected) mode and therefore do not contribute to readout noise. However, $N_m - 1$ dephased spin waves will emit read photons into all directions and therefore generate noise in the read mode [39,40]. Nonperfect rephasing of the readout mode adds additional noise proportional to $1 - p^{\mathrm{int}}_{r|w}$, where $p^{\mathrm{int}}_{r|w}$ is the intrinsic readout efficiency. We obtain the following expression for the total probability to detect a noise photon from dephased spin waves [40]:

$$p^{\mathrm{noise}}_{r|w} = p(N_{\mathrm{m}} - p^{\mathrm{int}}_{r|w})\frac{\beta_r}{\beta_w}\xi_{eg}\eta_r. \tag{2}$$

Here, p is the probability to generate a spin wave–write photon pair, $\beta_{w(r)}$ is the fraction of write (read) photons that are emitted into the collected spatial mode, ξ_{eg} is the branching ratio corresponding to the $|e\rangle - |g\rangle$ transition, and η_r is the detection efficiency of the read photons. In order to decrease this noise one can increase the ratio β_w of excitations paired with write photons over excitations paired with photons emitted into other spatial modes. This is achieved with an optical cavity enhancing the photon emission into the write photon spatial mode. Such a cavity is schematically described in Fig. 1(a). In order to not simultaneously increase β_r while increasing β_w, the read photon has orthogonal polarization from the cavity mode and is decoupled from the cavity by a polarization beam splitter (PBS).

Figure 2(a) characterizes the cavity-enhanced write photon emission. The cavity resonance frequency is changed by moving one of the cavity mirrors with a piezoelectric device. When the cavity resonance matches the write photon transition, photon emission is enhanced. However, when the two frequencies differ by more than the cavity linewidth, the emission is suppressed. At resonance we observe enhancement of $p^c_{\mathrm{enh}}/p = 14.3(6)$. Here, $p^c(p)$ is the write photon emission probability with (without) cavity. This is close to the expected value of $2F/\pi$ [45], while out of resonance inhibition is $p^c_{\mathrm{inh}}/p = 0.078(3)$. The spectral width of the emission is 16.6 MHz and matches the cavity linewidth (for more details on the cavity parameters, see Ref. [40]). Note that the effective enhancement of the write photon detection probability with cavity is reduced by the cavity escape efficiency, which for our implementation is 56%.

As mentioned before, the cavity enhancement of the write process allows for suppression of the read photon noise generated from dephased excitations. This is quantified in Figs. 2(b) and 2(c). In order to measure this dephased noise, a magnetic field gradient is applied during writing without field inversion before readout. This causes

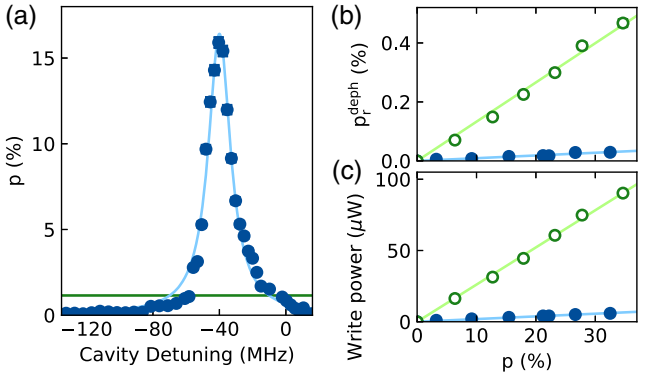

FIG. 2. (a) Write photon emission probability as a function of the cavity resonance frequency. Frequency zero corresponds to the center of the $|e\rangle - |s\rangle$ transition. The green solid line represents the emission without cavity enhancement. (b) Read photon detection probability from dephased spin waves and (c) write pulse power as a function of the spin wave excitation probability. The spin wave is read out after 1.2 μs of storage time. This time is much longer than the spin wave dephasing time set by the B field gradient [35]. Blue (green) data are taken with (without) cavity enhancement.

a rapid dephasing of the generated spin waves, and hence, all the readout photons are generated through interaction of the read pulse with dephased spin waves. In Fig. 2(b) [Fig. 2(c)], the read photon detection probability (write pulse power) is shown as a function of the write photon generation probability p. We observe that for the same excitation probability, the noise (write pulse power) is 14.4(7) [13.9(3)] times lower in the cavity-enhanced situation [which is compatible with the cavity enhancement observed in Fig. 2(a)]. The enhancement gives an approximate upper bound on the number of modes that can be used in a temporally multiplexed operation of the system.

After characterizing cavity-enhanced emission and noise reduction, we now compare temporally multiplexed storage with and without enhancement, as depicted in Fig. 1(c). Figure 3 shows a situation in which 6 write pulse modes are sent to the atomic cloud. In Fig. 3(a), after the six-modes write process, the magnetic field gradient is reversed. Upon detection of a write photon, we use a feed forward instruction in order to scan the readout around the expected rephasing time. We observe 6 peaks corresponding to the rephasing of each of the 6 spin wave modes. This figure shows 6 different datasets (separated with white and gray backgrounds) corresponding to write photon detection in different temporal modes. The ratio between the SNR achieved with or without cavity enhancement of ≈ 14 highlights the noise reduction achieved with cavity. For the cavity case, Fig. 3(b) characterizes the cross-correlation function between the write and read photons [defined as $g^{(2)}_{w,r} = p_{w,r}/(p_w p_r)$, where $p_{w,r}$ is the probability to detect a coincidence between write and read photon and $p_w(p_r)$ is the probability to detect a write (read) photon] in all the

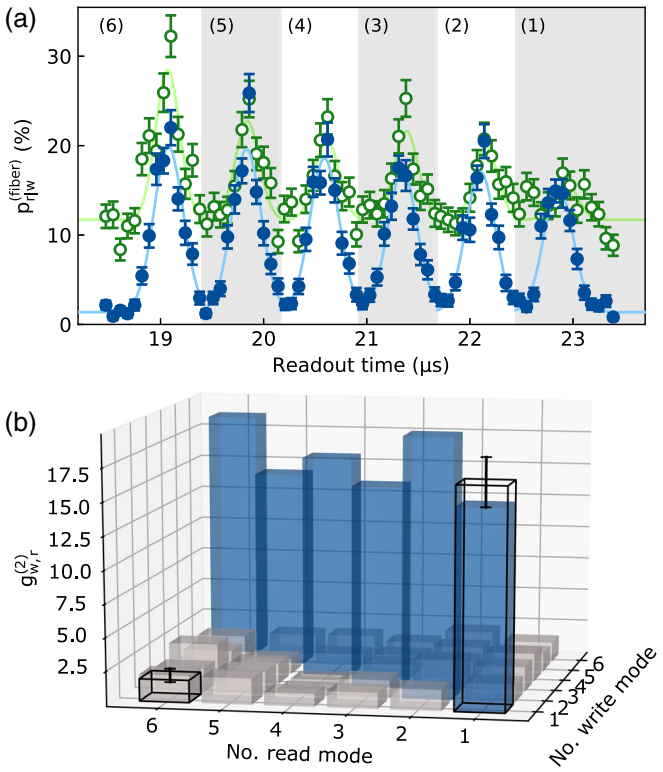

FIG. 3. (a) Probability to collect a heralded read photon into the read fiber as a function of the readout time for 6 different temporal modes. Time zero corresponds to time of writing of the last write mode (6). With cavity enhancement, intrinsic retrieval efficiency for the first mode is $p^{\mathrm{int}}_{r|w} \approx 26\%$. Blue (green) data are taken with (without) cavity enhancement. For both, single-mode excitation probability is $p_{1m} \approx 0.04$. Solid lines are a Gaussian fit of each retrieval peak. (b) Individual cross-correlation function between the different 6 write and read modes with cavity. The two bars in solid black lines at positions (1,1) and (1,6) represent the average for the diagonal and the off-diagonal values, respectively.

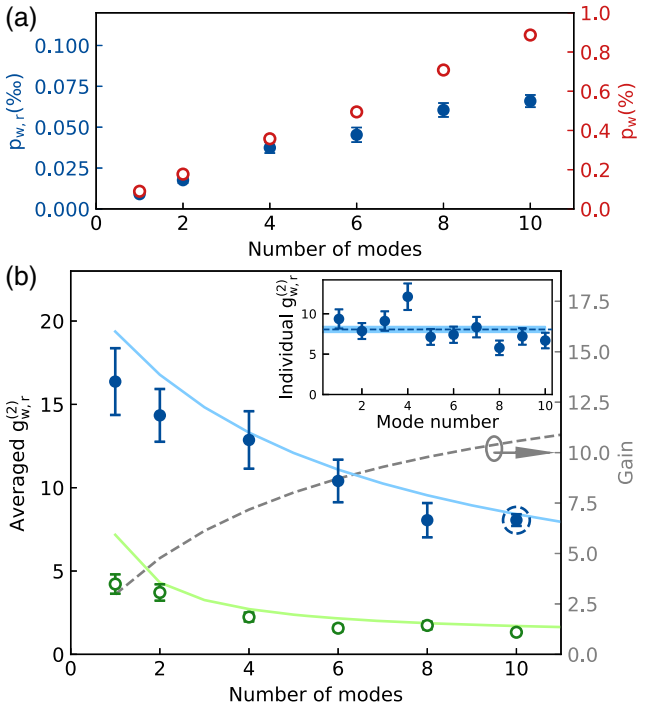

FIG. 4. (a) Write and total write-read detection probability as a function of the number of temporal modes with cavity. (b) Averaged correlation function between write and read photons as a function of the number of modes. Average is computed based on the sum of coincidence and noise counts from all modes. The error bar represents one standard deviation, again based on the sum of counts in all modes. Blue (green) data are taken with (without) cavity enhancement. Gray dashed line shows the gain $(g^{(2),c}_{w,r} - 1)/(g^{(2)}_{w,r} - 1)$ in cross-correlation enabled by the cavity, as a function of the number of modes. Here, $g^{(2),c}_{w,r}$ ($g^{(2)}_{w,r}$) is the cross-correlation value with (without) cavity. Inset shows $g^{(2)}_{w,r}$ of each mode for the ten-mode data point. Single-mode excitation probability is $p_{1m} \approx 0.045$ for all measurements.

36 possible combinations of six write and six read modes. The correlations are preserved when the read mode corresponds to the write mode [weighted average 16.6(1.8)]. However, little cross talk is observed when the read mode is different from the considered write mode [weighted average 1.7(0.5)].

Finally, we characterize the cavity-enhanced temporally multiplexed operation of the system. After a train of N_m write pulses and the recording of a write photon, the magnetic field gradient is inverted. A read pulse is sent at the expected rephasing time of its paired spin excitation. In Fig. 4(a), scanning the number of modes, we observe that the write photon detection probability per write pulse train, and hence the probability to create a spin wave–photon pair, increases linearly with N_m, while the write-read photon coincidence detection probability has a slightly worse scaling. This can be explained by the reduced readout efficiency as a function of storage time and by magnetic field fluctuations (cf. Ref. [40]). Nevertheless, for 10 modes we obtain a total rate enhancement of 7.3. In Fig. 4(b), again scanning N_m, we show the averaged value of $g^{(2)}_{w,r}$ across N_m modes. We notice that the multiplexed operation has a much stronger degradation impact on the correlation between the write and read photons when no cavity is present. The cavity significantly reduces the impact of the dephased spin waves on the quality of the correlations. It is also remarkable that $g^{(2)}_{w,r}$ is higher with cavity enhancement in the case of just 1 temporal mode. This highlights the imperfect rephasing of the spin wave, leading to dephased noise that is suppressed by the cavity. This is predicted by Eq. (2) for readout efficiencies < 1 and explained in more detail in Ref. [40]. Moreover, the values $g^{(2)}_{w,r} > 2$ are an evidence of quantum correlation between the write and read photons, assuming thermal statistics for the individual write and read modes. For 10 modes, we also measured the averaged heralded autocorrelation of the generated single photon

and found $g^{(2)}_{r,r|w} = 0.36(0.25) < 1$, confirming the nonclassical nature of the emitted photons.

The maximal number of temporal modes is currently limited by the finesse of our cavity, which is in turn limited by the optical intracavity loss, mostly given by the windows of our vacuum chamber. This loss is also responsible for the low escape efficiency in our current experiment (cf. Ref. [40]). This is, however, not a fundamental limitation. By implementing a cavity inside the vacuum chamber, a much higher cavity finesse could be achieved while keeping a high escape efficiency, such that $N_m > 100$ should be readily possible. For such a large number of modes, the next limitation is the spin wave storage time. With write modes separated by 800 ns as in our implementation, memory lifetimes of 2×80 μs become necessary. However, DLCZ experiments with cold atoms in optical lattices have shown much longer storage times of up to 200 ms [5,9]. Reaching long storage times is facilitated by the use of magnetically insensitive transitions to minimize decoherence by magnetic fluctuations. These transitions are not directly compatible with the broadening using magnetic gradients as demonstrated in our current proof of principle experiment. However, several solutions could be applied, e.g., transferring the excitations to clock transitions after the write pulse train [46] or using light shifts for inducing and reversing the broadening [47,48]. Finally, we note that the gain in coincidence count rate due to the multimode operation is only present for a fixed repetition rate of the experiment. This is, for example, the case for quantum repeater applications, where entanglement between distant quantum memories must be heralded. In that situation, the repetition rate of the entanglement attempts is limited to $R = c/L_0$, where L_0 is the distance between the ensembles. For example, for $L = 100$ km, $R = 2$ kHz. In that case, temporal multiplexing would increase the entanglement rate by a factor N_m for low success probability [3].

In conclusion, we presented a temporally multiplexed quantum repeater node based on cold atomic ensembles. By implementing a controlled inhomogeneous broadening of the spin transition, we generated distinguishable spin waves. We significantly reduced noise due to dephased spin waves by embedding the ensemble inside a low finesse optical cavity. This allowed us to demonstrate multiplexed generation of nonclassical spin wave–photon pairs in up to 10 temporal modes, enabling a corresponding increase in generation rate. These correlated pairs could also serve as a source of high-dimensional light-matter entanglement in time. The multiplexing capability can be further enhanced by using a higher finesse cavity or by combining temporal multiplexing with other techniques such as frequency or spatial multiplexing.

We acknowledge support by the Spanish Ministry of Economy and Competitiveness (MINECO) and the Fondo Europeo de Desarrollo Regional (FEDER) through Grant No. FIS2015-69535-R, by MINECO Severo Ochoa through Grant No. SEV-2015-0522, by the Gordon and Betty Moore Foundation through Grant No. GBMF7446 to H. d. R., by Fundaciós Privadas Cellex and and Mir-Puig and by the CERCA programme of the Generalitat de Catalunya. P. F. acknowledges financial support by the Cellex ICFO MPQ research fellowship program. L. H. acknowledges funding from the European Union's Horizon 2020 research and innovation programme under the Marie Skłodowska-Curie Grant Agreement No. 713729.

*Corresponding author.
lukas.heller@icfo.eu
†Corresponding author.
pau.farrera@icfo.eu
Present address: Max-Planck-Institut für Quantenoptik, Hans-Kopfermann-Strasse 1, 85748 Garching, Germany.
‡Present address: TOPTICA Projects GmbH, Lochhamer Schlag 19, 82166 Gräfelfing, Germany.
§http://qpsa.icfo.es

[1] F. Bussières, N. Sangouard, M. Afzelius, H. de Riedmatten, C. Simon, and W. Tittel, J. Mod. Opt. **60**, 1519 (2013).
[2] N. Sangouard, C. Simon, H. de Riedmatten, and N. Gisin, Rev. Mod. Phys. **83**, 33 (2011).
[3] C. Simon, H. de Riedmatten, M. Afzelius, N. Sangouard, H. Zbinden, and N. Gisin, Phys. Rev. Lett. **98**, 190503 (2007).
[4] E. Bimbard, R. Boddeda, N. Vitrant, A. Grankin, V. Parigi, J. Stanojevic, A. Ourjoumtsev, and P. Grangier, Phys. Rev. Lett. **112**, 033601 (2014).
[5] S.-J. Yang, X.-J. Wang, X.-H. Bao, and J.-W. Pan, Nat. Photonics **10**, 381 (2016).
[6] Y.-W. Cho, G. T. Campbell, J. L. Everett, J. Bernu, D. B. Higginbottom, M. T. Cao, J. Geng, N. P. Robins, P. K. Lam, and B. C. Buchler, Optica **3**, 100 (2016).
[7] P. Vernaz-Gris, K. Huang, M. Cao, A. S. Sheremet, and J. Laurat, Nat. Commun. **9**, 363 (2018).
[8] Y. Wang, J. Li, S. Zhang, K. Su, Y. Zhou, K. Liao, S. Du, H. Yan, and S.-L. Zhu, Nat. Photonics **13**, 346 (2019).
[9] A. G. Radnaev, Y. O. Dudin, R. Zhao, H. H. Jen, S. D. Jenkins, A. Kuzmich, and T. A. B. Kennedy, Nat. Phys. **6**, 894 (2010).
[10] L.-M. Duan, M. D. Lukin, J. I. Cirac, and P. Zoller, Nature (London) **414**, 413 (2001).
[11] C. W. Chou, H. de Riedmatten, D. Felinto, S. V. Polyakov, S. J. van Enk, and H. J. Kimble, Nature (London) **438**, 828 (2005).
[12] C.-W. Chou, J. Laurat, H. Deng, K. S. Choi, H. de Riedmatten, D. Felinto, and H. J. Kimble, Science **316**, 1316 (2007).
[13] Y.-A. Chen, S. Chen, Z.-S. Yuan, B. Zhao, C.-S. Chuu, J. Schmiedmayer, and J.-W. Pan, Nat. Phys. **4**, 103 (2008).
[14] S.-Y. Lan, A. G. Radnaev, O. A. Collins, D. N. Matsukevich, T. A. Kennedy, and A. Kuzmich, Opt. Express **17**, 13639 (2009).
[15] A. Nicolas, L. Veissier, L. Giner, E. Giacobino, D. Maxein, and J. Laurat, Nat. Photonics **8**, 234 (2014).

[16] D.-S. Ding, W. Zhang, Z.-Y. Zhou, S. Shi, G.-Y. Xiang, X.-S. Wang, Y.-K. Jiang, B.-S. Shi, and G.-C. Guo, Phys. Rev. Lett. **114**, 050502 (2015).
[17] Y.-F. Pu, N. Jiang, W. Chang, H.-X. Yang, C. Li, and L.-M. Duan, Nat. Commun. **8**, 15359 (2017).
[18] R. Chrapkiewicz, M. Dąbrowski, and W. Wasilewski, Phys. Rev. Lett. **118**, 063603 (2017).
[19] M. Parniak, M. Dąbrowski, M. Mazelanik, A. Leszczyński, M. Lipka, and W. Wasilewski, Nat. Commun. **8**, 2140 (2017).
[20] L. Tian, Z. Xu, L. Chen, W. Ge, H. Yuan, Y. Wen, S. Wang, S. Li, and H. Wang, Phys. Rev. Lett. **119**, 130505 (2017).
[21] M. Afzelius, C. Simon, H. de Riedmatten, and N. Gisin, Phys. Rev. A **79**, 052329 (2009).
[22] H. de Riedmatten, M. Afzelius, M. U. Staudt, C. Simon, and N. Gisin, Nature (London) **456**, 773 (2008).
[23] I. Usmani, M. Afzelius, H. de Riedmatten, and N. Gisin, Nat. Commun. **1**, 12 (2010).
[24] C. Clausen, I. Usmani, F. Bussières, N. Sangouard, M. Afzelius, H. de Riedmatten, and N. Gisin, Nature (London) **469**, 508 (2011).
[25] E. Saglamyurek, N. Sinclair, J. Jin, J. A. Slater, D. Oblak, F. Bussières, M. George, R. Ricken, W. Sohler, and W. Tittel, Nature (London) **469**, 512 (2011).
[26] M. Gündoğan, P. M. Ledingham, K. Kutluer, M. Mazzera, and H. de Riedmatten, Phys. Rev. Lett. **114**, 230501 (2015).
[27] A. Tiranov *et al.*, Phys. Rev. Lett. **117**, 240506 (2016).
[28] P. Jobez, N. Timoney, C. Laplane, J. Etesse, A. Ferrier, P. Goldner, N. Gisin, and M. Afzelius, Phys. Rev. A **93**, 032327 (2016).
[29] A. Seri, A. Lenhard, D. Rieländer, M. Gündoğan, P. M. Ledingham, M. Mazzera, and H. de Riedmatten, Phys. Rev. X **7**, 021028 (2017).
[30] K. Kutluer, M. Mazzera, and H. de Riedmatten, Phys. Rev. Lett. **118**, 210502 (2017).
[31] C. Laplane, P. Jobez, J. Etesse, N. Gisin, and M. Afzelius, Phys. Rev. Lett. **118**, 210501 (2017).
[32] T.-S. Yang *et al.*, Nat. Commun. **9**, 3407 (2018).
[33] M. Hosseini, B. M. Sparkes, G. Campbell, P. K. Lam, and B. C. Buchler, Nat. Commun. **2**, 174 (2011).
[34] Q. Glorieux, J. B. Clark, A. M. Marino, Z. Zhou, and P. D. Lett, Opt. Express **20**, 12350 (2012).
[35] B. Albrecht, P. Farrera, G. Heinze, M. Cristiani, and H. de Riedmatten, Phys. Rev. Lett. **115**, 160501 (2015).
[36] P. Farrera, G. Heinze, and H. de Riedmatten, Phys. Rev. Lett. **120**, 100501 (2018).
[37] Y. Wen, P. Zhou, Z. Xu, L. Yuan, H. Zhang, S. Wang, L. Tian, S. Li, and H. Wang, Phys. Rev. A **100**, 012342 (2019).
[38] C. Li *et al.*, arXiv:1909.02185.
[39] C. Simon, H. de Riedmatten, and M. Afzelius, Phys. Rev. A **82**, 010304(R) (2010).
[40] See Supplemental Material at http://link.aps.org/supplemental/10.1103/PhysRevLett.124.210504 for details, which include Refs. [41–44].
[41] P. Farrera, N. Maring, B. Albrecht, G. Heinze, and H. de Riedmatten, Optica **3**, 1019 (2016).
[42] X. Bao, A. Reingruber, P. Dietrich, J. Rui, A. Dück, T. Strassel, L. Li, N.-L. Liu, B. Zhao, and J.-W. Pan, Nat. Phys. **8**, 517 (2012).
[43] H. de Riedmatten, J. Laurat, C. W. Chou, E. W. Schomburg, D. Felinto, and H. J. Kimble, Phys. Rev. Lett. **97**, 113603 (2006).
[44] J. Simon, H. Tanji, J. K. Thompson, and V. Vuletic, Phys. Rev. Lett. **98**, 183601 (2007).
[45] C. W. Wilmsen, H. Temkin, and L. A. Coldren, *Vertical-Cavity Surface-Emitting Lasers: Design, Fabrication, Characterization, and Applications*, *Cambridge Studies in Modern Optics* (Cambridge University Press, Cambridge, England, 1999).
[46] Y. Jiang, J. Rui, X.-H. Bao, and J.-W. Pan, Phys. Rev. A **93**, 063819 (2016).
[47] B. M. Sparkes, M. Hosseini, G. Hétet, P. K. Lam, and B. C. Buchler, Phys. Rev. A **82**, 043847 (2010).
[48] M. Parniak, M. Mazelanik, A. Leszczyński, M. Lipka, M. Dąbrowski, and W. Wasilewski, Phys. Rev. Lett. **122**, 063604 (2019).